HHS Public Access

Author manuscript

Nature. Author manuscript; available in PMC 2011 May 11.

Published in final edited form as:

Nature. 2010 November 11; 468(7321): 305–309. doi:10.1038/nature09511.

Reducing excessive GABAergic tonic inhibition promotes post-stroke functional recovery

Andrew N. Clarkson[1,4,*], **Ben S. Huang**[1,2,*], **Sarah E. MacIsaac**[1], **Istvan Mody**[1,2,3], and **S. Thomas Carmichael**[1]

[1]Department of Neurology, The David Geffen School of Medicine at UCLA, 635 Charles Young Drive South, Los Angeles, California, USA

[2]Interdepartmental Ph.D.Program for Neuroscience, The David Geffen School of Medicine at UCLA, 635 Charles Young Drive South, Los Angeles, California, USA

[3]Department of Physiology, The David Geffen School of Medicine at UCLA, 635 Charles Young Drive South, Los Angeles, California, USA

Abstract

Stroke is a leading cause of disability; but no pharmacological therapy is currently available for promoting recovery. The brain region adjacent to stroke damage, the peri-infarct zone, is critical for rehabilitation, as it exhibits heightened neuroplasticity, allowing sensorimotor functions to re-map from damaged areas1–3. Thus, understanding the neuronal properties constraining this plasticity is important to developing new treatments. Here we show that after a stroke in mice, tonic neuronal inhibition is increased in the peri-infarct zone. This increased tonic inhibition is mediated by extrasynaptic $GABA_A$ receptors ($GABA_A$Rs) and is caused by an impairment in GABA transporter (GAT-3/4) function. To counteract the heightened inhibition, we administered *in vivo* a benzodiazepine inverse agonist specific for the α5-subunit-containing extrasynaptic $GABA_A$Rs at a delay after stroke. This treatment produced an early and sustained recovery of motor function. Genetically lowering the number of α5 or δ-subunit-containing $GABA_A$Rs responsible for tonic inhibition also proved beneficial for post-stroke recovery, consistent with the therapeutic potential of diminishing extrasynaptic $GABA_A$R function. Together, our results identify new pharmacological targets and provide the rationale for a novel strategy to promote recovery after stroke and possibly other brain injuries.

Correspondence and requests for materials should be addressed to S.T.C. (scarmichael@mednet.ucla.edu)..

[4]Present address: Departments of Psychology and Anatomy and Structural Biology, University of Otago, PO Box 913, Dunedin 9013, New Zealand.

*These authors contributed equally to this work.

Author Contributions: A.N.C. performed the behavioral, histological and immunohistochemical studies; B.S.H. carried out the electrophysiological experiments; and S.E.M. performed the immunohistochemical and Western blot work. A.N.C, B.S.H., I.M. and S.T.C. designed the experiments, analyzed data, prepared figures, and wrote the manuscript.

Supplementary Information: Supplementary information includes Supplementary Methods, Figures, including a Supplementary Figure 1 summarizing the main result and accompanies this paper on www.nature.com/nature.

Author Information:: Reprints and permissions information is available at npg.nature.com/reprintsandpermissions. The authors have no competing financial interests to declare.

Stroke is a major source of disability, confining one-third of stroke survivors to nursing homes or institutional settings4. Recent studies have shown that the brain has a limited capacity for repair after stroke. Neural repair after stroke involves re-mapping of cognitive functions in tissue adjacent to or connected with the stroke5,6. Functional recovery in this peri-infarct tissue involves changes in neuronal excitability that alter the brain's representation of motor and sensory functions. Stimulation of peri-infarct cortex enhances local neuronal excitability through a process that involves long-term potentiation (LTP), alters sensorimotor maps, and improves use of affected limbs5–8. The inhibitory neurotransmitter GABA is critical for cortical plasticity and sensory mapping. Altering GABAergic transmission changes sensory maps during the critical period of cortical development9 and produces rapid alterations in adult cortical maps that resemble changes occurring after stroke10,11. Alterations in cortical maps through blockade of GABAergic signaling are associated with fundamental changes in cellular excitability including LTP12. In a similar manner to normal cortical plasticity, GABAergic mechanisms may mediate changes in neuronal excitability that play a central role in functional recovery of peri-infarct cortex after stroke.

Cortical GABAergic signaling through $GABA_A$Rs is divided into synaptic (phasic) and extrasynaptic (tonic) components. Tonically active extrasynaptic $GABA_A$Rs set an excitability threshold for neurons13,14. Extrasynaptic $GABA_A$Rs primarily consist of α5 or δ-subunit-containing receptors13,14. Pharmacological and genetic knockdown of α5-$GABA_A$Rs enhance LTP and improve performance on learning and memory tasks15,16. The selective effects of extrasynaptic $GABA_A$Rs on cellular excitability and plasticity, and the evidence that changes in neuronal excitability underlie functional reorganization in peri-infarct cortex, suggest that this system may play a role in post-stroke recovery. We find that stroke increases tonic GABAergic transmission in peri-infarct cortex and dampening this tonic inhibition produces an early and robust gain of motor recovery post-stroke (Supplementary Fig. 1, schematic summary).

We examined neuronal excitability in the peri-infarct cortex of mice during the period of recovery and reorganization after a photothrombotic stroke to forelimb motor cortex. Whole-cell voltage-clamp recordings in *in vitro* brain slices prepared at 3-, 7-, and 14-days post-stroke (Fig. 1a) showed a significant increase in $GABA_A$R-mediated tonic inhibition (I_{tonic}) in layer 2/3 pyramidal neurons, compared to neurons from sham controls (control: 8.05±0.80 pA/pF, n=24, *vs*. post-stroke: 13.6±1.41 pA/pF, n=45, Mann-Whitney U-test, P<0.05; Fig. 1b). I_{tonic} remained elevated from 3- to 14-days post-stroke (Supplementary Fig. 2a). The mean phasic excitation remained unchanged over the 2-week period after stroke (Supplementary Fig. 3a, b). The mean phasic inhibition was unchanged except for a transient decrease at 7-days post-stroke (Supplementary Fig. 3c, d). The resting membrane and GABA reversal potentials were both unchanged (Supplementary Fig. 3e, f).

Tonic inhibition is effectively controlled by the degree of extracellular GABA uptake through neuronal and astrocytic GABA transporters (GATs)14. We applied a GAT-1-selective antagonist, NO-711 (10μM), and found a significantly greater effect (% I_{tonic} increase after GAT blockade) in post-stroke neurons (94.0±16.3%, n=10) than in controls (34.3±11.4%, n=6; P<0.05; Fig. 2a). Co-application of NO-711 and the GAT-3/4-selective

antagonist SNAP-5114 (40 μM) produced a substantial increase in I_{tonic} in controls (300.6±46.0%, *n*=4; Fig. 2a), revealing the synergistic actions of GATs in the cortex as previously proposed17. In post-stroke neurons, co-application only produced an effect (110.7±32.0%, *n*=5) similar to GAT-1 blockade alone (*P*=0.68; Fig. 2a), indicating a dysfunction in GAT-3/4 after stroke. Sequential blockade of the two GATs confirmed the post-stroke impairment, as peri-infarct I_{tonic} showed no further response to GAT-3/4 blockade after the initial GAT-1 block, in contrast to responses shown in controls (Fig. 2b, c). This effect was not due to receptor saturation, as I_{tonic} showed further increase in response to raised [GABA] under GAT blockade (Supplementary Fig. 4a). Western-blot analysis confirmed a reduced GAT-3/4 level in peri-infarct cortex, whereas GAT-1 levels were unchanged (Supplementary Fig. 5).

We hypothesized that the chronically elevated tonic inhibition in the peri-infarct region may antagonize the neuronal plasticity required for functional recovery after stroke. Therefore, we tested whether reducing the excessive tonic inhibition would improve function recovery. Of the two $GABA_A$Rs subtypes shown to underlie tonic inhibition in cortical neurons, the α5-$GABA_A$Rs can be antagonized specifically by L655,708, a benzodiazepine inverse agonist16, while no specific antagonist exists for δ-$GABA_A$Rs. L655,708 (100 nM) decreased I_{tonic} in control neurons by −13.3±5.2% (*n*=4), but produced a significantly greater decrease in post-stroke neurons (−30.0±4.1%, *n*=13; *P*<0.05; Fig. 2d, e), which reverted I_{tonic} back to control level (control: see above *vs*. post-stroke + L655,708: 140.8±18.5pA, *n*=13; *P*=0.702; Fig. 2f). L655,708 produced only minimal effects on phasic inhibitory currents in both post-stroke and control conditions (Supplementary Fig. 4b).

We next tested the effects of reducing tonic inhibition on functional recovery after stroke, using measures of fore- and hindlimb motor control. Stroke produced an increase in the number of foot-faults in grid-walking task, and a decrease in forelimb asymmetry in the cylinder task from 7-days post-stroke. Chronic treatment with L655,708 starting 3-days post-stroke resulted in a dose-dependent maximal gain of function beginning from 7-days post-stroke in both tasks (*P*<0.001; Fig. 3a–c). Acute treatment with L655,708 just prior to behavioral testing had a minimal effect on stroke recovery (Supplementary Fig. 7). To assess the necessity of long-term administration, we discontinued L655,708 treatment after 2 weeks and found a decrease in functional gains, although these mice still performed better than vehicle-treated stroke controls (Supplementary Fig. 6).

To further corroborate the role of reduced tonic inhibition in enhancing stroke recovery, we tested mice with deletions of either α5 or δ-subunit-containing $GABA_A$Rs ($Gabra5^{-/-}$ and $Gabrd^{-/-}$, Methods)18. $Gabra5^{-/-}$ animals showed significantly better motor recovery post-stroke, comparable to L655,708-treated wild-type animals (Fig. 3d–f). In addition, $Gabra5^{-/-}$ animals displayed a significant reduction in hindlimb foot-faults (Fig. 3e). $Gabrd^{-/-}$ animals also showed significant improvements in motor recovery (Fig. 3d–f), but to a lesser extent than the $Gabra5^{-/-}$ mice. Thus, modulation of α5$GABA_A$Rs affords greater functional gains in motor recovery than δ$GABA_A$Rs, and genetic removal of α5$GABA_A$Rs produces a more widespread increase in motor recovery than pharmacological antagonism. Administration of L655,708 to $Gabrd^{-/-}$ mice produced an even greater

recovery, confirming the beneficial effect of reducing peri-infarct tonic inhibition (Fig. 3a, c).

Low/sub-seizure dosing of picrotoxin (PTX: 0.1mg/kg, i.p.), a use-dependent $GABA_AR$ antagonist, enhances learning and memory in transgenic mouse models of Alzheimer's and other cognitive impairments by reversing an increased GABAergic inhibitory tone, acting at both synaptic and extrasynaptic $GABA_ARs$19,20. The pharmacological effects of PTX on reducing phasic and tonic inhibition were not altered after stroke (Supplementary Table II). PTX given to animals from 3-days post-stroke resulted in a significant gain of forelimb function on the grid-walking task compared to vehicle-treated stroke controls ($P<0.05$; Supplementary Fig. 9a). No significant changes were observed in hindlimb function or forelimb asymmetry (Supplementary Fig. 9b, c). Combined L655,708 + PTX treatment showed similar initial functional gains compared to stroke + L655,708 alone; however, prolonged PTX + L655,708 treatment produced a deterioration in motor function such that the performance progressively worsened at late periods after stroke (Supplementary Fig. 9). These data suggest that increasing cortical excitability too far or reducing phasic inhibition negatively impact functional recovery.

An important element in stroke treatment is the timing of drug delivery. $GABA_AR$ agonists administered at the time of stroke decrease stroke size20. Therefore, dampening tonic inhibition too early after stroke may produce an opposite effect, i.e. increased cell death. To test this, we assessed stroke volume at 7-days post-stroke, in animals treated with 1) vehicle, 2) L655,708 from stroke onset, and 3) L655,708 from day-3 post-stroke. Stroke volumes were similar between mice treated with vehicle and L655,708 from day-3 (Fig. 4). In contrast, stroke volume was significantly increased in animals treated with L655,708 from stroke onset ($P<0.05$; Fig. 4). These data indicate a critical timeframe for therapeutically dampening tonic inhibition post-stroke: reduction too early would exacerbate stroke damage, while delaying treatment by 3-days would promote functional recovery without altering stroke size. Genetic deletion of α5- or δ- $GABA_ARs$ did not affect infarct size or neuronal number in peri-infarct cortex (Supplementary Fig. 8). Unlike pharmacological antagonism of α5-$GABA_AR$-mediated inhibition, in Gabra5$^{-/-}$ and Gabrd$^{-/-}$ mice, the genomic absence of one of the extrasynaptic $GABA_ARs$ may trigger compensatory upregulation of the other receptor13 and thus obscuring their roles in neuroprotection immediately after stroke.

Current therapies that promote functional recovery after stroke are limited to physical rehabilitation4. Here, by identifying an excessive tonic inhibition after stroke, we have found promising new targets for pharmacological interventions to promote recovery. The elevated tonic inhibition in cortical pyramidal neurons occurs during precisely the same time-period important for cortical map plasticity and recovery1–3. Alterations in other aspects of cortical signaling have also been described during this period, including altered $GABA_AR$ subunits, glutamate receptor expression and neuronal network properties21–24. Protein levels of GAT-1 and GAT-3/4 were shown to be decreased in peri-infarct cortex in some rodent stroke models, and reactive astrocytes exhibit reduced uptake of other neurotransmitters23. However, there are conflicting data on $GABA_AR$ levels after stroke23–26. We found decreased protein level and compromised function of GAT-3/4 in peri-infarct cortex. The elevated tonic inhibition may curtail cortical plasticity and spontaneous recovery

after stroke, and is consistent with tonic GABAergic inhibition exerting a causal role in limiting motor recovery in stroke.

Non-selectively decreasing GABAergic tone facilitates neuronal plasticity in genetic models of cognitive diseases19,20. We show for the first time that antagonizing an elevated tonic inhibition enhances motor recovery after stroke, consistent with the idea that molecular and cellular events of neuronal plasticity are dampened in the peri-infarct zone, and promoting this plasticity facilitates functional recovery. Together, our results have identified novel pharmacological targets and provide a rational basis for developing future therapies to promote recovery after stroke and possibly other brain injuries.

Methods Summary

Photothrombotic model of focal stroke

Focal stroke was induced by photothrombosis in adult male C57BL/6 mice (age 2–4 month) as described by27.

Slice preparation for electrophysiology

Following decapitation, brains were rapidly removed and placed into a *N*-methyl-D-glucamine (NMDG)-based cutting solution to enhance neuronal viability28. Coronal slices (350μm) were cut and transferred to an interface-style chamber containing artificial cerebrospinal fluid as previously described13. Recordings were made from intact peri-infarct cortical layer-2/3 pyramidal neurons and analyzed as previously described13.

*In vivo*drug administration

L655,708 was dissolved in DMSO and then diluted 1:1 in 0.9% saline. L655,708-filled ALZET-1002 pumps were implanted at 3-days post-stroke and replaced every two weeks. In acute administration studies, 5mg/kg L655,708 was administered (i.p.) 30 minutes prior to testing. The concentration in one minipump, 5mM, delivers a 200ug/kg/day dose in mice. With one or two minipumps implanted, this provides a dose escalation. PTX (0.1mg/kg i.p. bi-daily) starting 3-days post-stroke was administered alone or in concert with L655,708.

Behavioral analysis

Mice were videotaped during walking and exploratory behavior in the grid-walking and cylinder/rearing tasks, tested at approximately the same time each day during the nocturnal period29. Baseline behavioral measurements were obtained one week prior to surgery. Post-stroke animals were assessed at weeks 1, 2, 4, and 6.

Infarct-size measurement—For the histological assessment of infarct size, brains were processed at 7-days post-stroke using cresyl violet as previously described30.

Statistical analysis—All data are expressed as mean ± s.e.m. For electrophysiological comparisons between control *vs*. post-stroke, Mann-Whitney non-parametric test was used. For multiple comparisons across post-stroke days, one-way analysis of variances (ANOVA) and Newman–Keuls' multiple pair-wise comparisons for post-hoc comparisons were used.

For behavioral testing, differences between treatment groups were analyzed using two-way ANOVA with repeated measures and Newman–Keuls' multiple pair-wise comparisons. The level of significance was set at $P<0.05$.

METHODS

Photothrombotic model of focal stroke—Under isoflurane anesthesia (2–2.5% in a 70% N_2O / 30% O_2 mixture), 2–4 month-old adult C57Bl6 (Charles River, Wilmington, MA) male mice were placed in a stereotactic apparatus, the skull exposed through a midline incision, cleared of connective tissue and dried. A cold light source (KL1500 LCD, Zeiss) attached to a 40× objective giving a 2mm diameter illumination was positioned 1.5mm lateral from Bregma, and 0.2mL of Rose Bengal solution (Sigma; 10 g/L in normal saline, i.p.) was administered. After 5-min, the brain was illuminated through the intact skull for 15-min. Rose-bengal produces singlet oxygen under light excitation, which damages and occludes vascular endothelium, resulting in focal cortical stroke under the region of illumination (Fig. 4), circumscribed by peri-infarct tissue with normal neuronal cell number (Supplementary Fig. 8). Two to four month-old adult male Gabra5$^{-/-}$ and Gabard$^{-/-}$ mice1 received stroke as above. These mice had been back-crossed to C57Bl6 in excess of 15 generations, and were compared in behavioral studies to wild-type C57Bl6. Body temperature was maintained at 36.9 ± 0.4°C with a heating pad throughout the operation and did not vary by drug or genetic condition. This stroke method produces a small stroke in the mouse forelimb region of the motor cortex (Fig. 4). Sample size was 10 per group for Gabara5−/− and Gabard−/− in stroke/behavioral studies. Sample size was 8 per group for each condition in dosing of L655,708 (Fig. 3).

Blood pressure (systolic and diastolic) and heart rate were measured in separate cohorts of mice in wild-type (C57Bl6), with and without L655,708 administration via ALZET minipumps from 3-days post-stroke, and in Gabra5$^{-/-}$ and Gabrd$^{-/-}$ mice, before during and after stroke, using a standard non-invasive tail-cuff method (Coda, Kent Scientific, Torrington, CT). There were no significant differences in heart rate or blood pressure by treatment or genotype (Supplementary Table I). All studies in this manuscript complied with the STAIR (*Stroke Therapy Academic Industry Roundtable*) criteria for stroke investigations in measuring physiological parameters, monitoring treatment effects for at least one month, analyzing treatment effects blinded to conditions, utilizing dose-response studies, and use of a drug administration route with blood brain barrier penetration.

Whole-cell voltage-clamp electrophysiology—Slices were submerged in the recording chamber and continuously perfused (5–8 ml/min) with oxygenated ACSF (32–34°C). Visualized patch-clamp recordings from layer-2/3 pyramidal neurons were performed at 40x using infra-red oblique-illumination (Leica DM-LFS; Hamamatsu CCD camera C3077–78).

Control recordings were made from cells of sham-operated animals at similar locations as those recorded in post-stroke animals. Microelectrodes (3–5 MΩ) were filled with a cesiummethylsulfonate ($CsMeSO_4$)-based internal pipette solution, containing (in mM) 120 $CsMeSO_4$, 10 CsCl, 5 TEA-Cl, 1.5 $MgCl_2$, 10 HEPES, 0.1 EGTA, 2 Na-ATP, 0.5 Na-GTP,

and 5 QX-314, pH 7.25–7.30 with CsOH, 275–285 mOsm. The recording ACSF was supplemented with 5 μM GABA to replenish the extracellular GABA concentration reduced by the high-flow perfusion of the slices1. For recording I_{tonic} at −70 mV, a high-CsCl-based internal solution was used, containing (in mM) 140 CsCl, 1 $MgCl_2$, 10 HEPES, 0.1 EGTA, 4 NaCl, 2 Mg-ATP, 0.3 Na-GTP, and 5 QX-314, pH ~7.3, ~275 mOsm/l, with ACSF containing 3 mM kynurenic acid to block glutamatergic currents.

Neurons were voltage-clamped in whole-cell configuration using a MultiClamp-700A amplifier (Molecular Devices); all recordings were low-pass-filtered at 3 kHz (8-pole Bessel) and digitized online at 10 kHz (National Instruments PCI-MIO-16E-4 board). Series resistance and whole-cell capacitance were estimated from fast transients evoked by a 5mV step and compensated to 75%. EPSCs and IPSCs were recorded by voltage-clamping sequentially at −70mV and +10mV, respectively. All drugs were purchased from Sigma or Tocris. L-655,708 and SNAP-5114 were dissolved in DMSO then diluted 1:1000 in H_2O. NO-711, Gabazine and GABA were dissolved in H_2O.

Tonic inhibitory current and mean phasic current determination—Custom-written macros running under IGOR Pro v.6.0 (WaveMetrics, Inc.) were used to analyze the digitized recordings to determine the values of tonic currents and mean phasic currents, as previously described1. I_{tonic} was recorded as the reduction in baseline holding currents (I_{hold}) after bath-applying a saturating amount (>100μM) of the $GABA_AR$ antagonist SR-95531 (gabazine), while voltage-clamping at +10mV. NO-711, SNAP-5114 and L-655,708 were added to the recording ACSF via perfusion and their effects on I_{tonic} were recorded as the post-drug shift in I_{hold}. Drug perfusion was continued until the shifting I_{hold} remained steady for 1–2 min.

To determine the mean phasic current (I_{mean}), a 60-s segment containing either EPSCs or IPSCs was selected, and an all-point histogram was plotted for every 10,000 points (every 1s), smoothed, and fitted with a Gaussian to obtain the mean baseline current. All baseline mean values were then plotted and linear trends subtracted to normalize the mean baseline current to 0pA. After baseline normalization, the values of each 10,000 points (each 1s) were averaged to yield the value of I_{mean} (in pA/s) for each 1s epoch. The averaged I_{mean} value of a 60s segment was reported as the phasic I_{mean} value for either the spontaneous EPSC or IPSC. Synaptic event kinetics (i.e. frequency, peak amplitude, 10–90% rise time, and weighted decay time constant) are analyzed by custom-written LabView-based software (EVAN), as previously described1. For comparison of the IPSC peak amplitudes under control and PTX-treated conditions (Supplementary Table II), the largest-amplitude count-matched method was used, whereby the amplitude values in a given recording were sorted and the largest x number of events under control condition were averaged and taken for comparison with the average of an equally-matched x number of events under the PTX condition, with x determined by the number of events detected under the 10 μM PTX condition. This method circumvents the erroneous comparison of average amplitudes when considering the effects of a receptor antagonist that reduces the smaller events (in control condition) below the noise level.

Measurements of neuronal resting membrane potential (V_{rest}) and GABA reversal potential (E_{GABA})—To estimate V_{rest}, the cell-attached recording technique2 was used. Briefly, depolarizing voltage ramps (−100 to +200 mV) were applied to cell-attached patches to activate voltage-gated K^+ channels and establish the K^+ current reversal potential, which provides a measure of the V_{rest}, given near equimolar K^+ inside the cell and the pipette. E_{GABA} was estimated by measuring the K^+ reversal potential after activating $GABA_A$Rs with 50μM muscimol. Recordings were made using a solution containing the following (in mM): K+ gluconate (135), KCl (5), $MgCl_2$ (2), HEPES (10), EGTA (0.1), Na-ATP (4), Na-GTP (0.3), pH 7.3, 273mOsm/l. A junction potential of 9mV was measured and then subtracted from voltage values of all measurements.

Fitting of multiple distributions to cumulative probability plots—The fitting of multiple distributions to a cumulative probability plot (Supplementary Fig. 2) was done as follows. Cumulative probabilities of the variable x (i.e., P(x)) were calculated and fitted by one or more normal curves approximated by the logistic equation3:

$$P(x) = \sum_{i=1}^{n} R_i \frac{x^{p_i}}{x^{p_i} + \bar{x}^{p_i}}$$

where $R_1, \ldots, R_n$ are the ratios of the n normal distributions (such as $\sum_{i=1}^{n} R_n = 1$), $\bar{x}_1, \ldots, \bar{x}_n$, are the individual means, and $p_1, \ldots, p_n$ are steepness factors related to the n standard deviations ($SD_1, \ldots SD_n$).

Behavioral analysis

Grid-walking Task—The grid-walking apparatus was manufactured as previously described4, using 12mm square wire mesh with a grid area 32cm / 20cm / 50cm (length / width / height). A mirror was placed beneath the apparatus to allow video footage in order to assess the animals' stepping errors (i.e. `footfaults'). Each mouse was placed individually atop of the elevated wire grid and allowed to freely walk for a period of 5min. Video footage was analyzed offline by raters blind as to the treatment groups. The total number of footfaults for each limb, along with the total number of non-footfault steps, was counted, and a ratio between footfaults and total-steps-taken calculated. Percent footfaults were calculated by: [#footfaults / (#footfaults + #non-footfault steps) * 100]. A ratio between footfaults and total steps taken was used to take into account differences in the degree of locomotion between animals and trials. A step was considered a footfault if it was not providing support and the foot went through the grid hole. Further, if an animal was resting with the grid at the level of the wrist, this was also considered a fault. If the grid was anywhere forward of the wrist area then this was considered as a normal step.

Spontaneous Forelimb Task (Cylinder Task)—The spontaneous forelimb task encourages the use of forelimbs for vertical wall exploration / press in a cylinder5. When placed in a cylinder, the animal rears to a standing position, whilst supporting its weight with either one or both of its forelimbs on the side of the cylinder wall. Animals were placed inside a Plexiglas cylinder (15cm in height with a diameter of 10cm was used) and

videotaped for 5min. Videotape footage of animals in the cylinder were evaluated quantitatively in order to determine forelimb preference during vertical exploratory movements. While the video footage was played in slow motion (1/5th real time speed), the time (sec) during each rear that each animal spent on either the right forelimb, the left forelimb, or on both forelimbs were calculated. Only rears in which both forelimbs could be clearly seen were timed. The percentage of time spent on each limb was calculated and these data were used to derive an SFL asymmetry index (% ipsilateral use- % contralateral use). The `contact time' method of examining the behavior was chosen over the `contact placement' method, as described by5, as it takes into account the slips that often occur during a bilateral wall press post-photothrombosis.

Western Blot—Seven days after stroke mice were decapitated, the brains rapidly removed and peri-infarct cortex microdissected and frozen (*n*=5). The equivalent region of cortex was taken in control, non-operated mice (*n*=3). Samples were homogenized in radioimmunoprecipitation (RIPA) buffer (Pierce; Rockford, IL) and centrifuged at 20000×g at 4°C for 10 minutes. Supernatant was collected as protein extract and stored at −80°C. Western blot was performed as described5. 100 ug of protein from each sample was diluted in 7.5 ul of 2× SDS- sample buffer gel (Invitrogen; Carlsbad, CA) containing dithiothreitol (DTT) (Sigma, St. Louis, MO) and brought to a final volume of 15 ul with RIPA buffer. Samples were denatured at 95°C, loaded on to a 4–12 % gradient Tris-Glycine gel (Invitrogen; Carlsbad, CA), separated via SDS-PAGE, and then transferred to HYBOND™-P (pvdf) membrane (Amersham; Piscataway, NJ) at 30 volts for 2 hours. Membranes were rinsed and blocked overnight at 4°C. Membranes probed with antibodies against GABA Transporter 3 (Rbt Anti-GAT-3 1:1000; Millipore; Temcula, CA), and GABA Transporter 1 (Rbt Anti-GAT-1 1:200; Millipore; Temecula, CA). Following successive washes, membranes were incubated in IgG Donkey Anti-Rabbit HRP-labeled secondary (1:6000; Jackson; West Grove, PA) for one hour at room temperature. Membranes were incubated in ECL PLUS (Amersham; Piscataaway, NJ)) and chemiluminescence was detected using Fluorochem (Alpha Innotech, San Leandro, CA). Membranes were then re-probed for one hour at room temperature with GAPDH (1:2500; Abcam; Cambridge, MA) and Donkey Anti-Rbt-HRP (1:10000; Jackson; West Grove, PA) as an endogenous control protein to ensure equal loading. Immunoblotting was performed in triplicate for each antibody. Adobe Photoshop software (Adobe Systems Inc, San Jose, CA) was used for densitometric analysis of all blots.

Supplementary Material

Refer to Web version on PubMed Central for supplementary material.

Acknowledgements

Supported by The Dr. Miriam and Sheldon G Adelson Medical Research Foundation, the Larry L. Hillblom Foundation (A.N.C., S.T.C.), the Coelho Endowment (I.M.) and NIH/NINDS grant NS30549 (I.M.). This manuscript was completed partially during tenure of an American Heart Association Postdoctoral Fellowship, a Repatriation Fellowship from the New Zealand Neurological Foundation and the Sir Charles Hercus Fellowship from the Health Research Council of New Zealand (A.N.C). We thank E.O. Mann, J. Chu, J.J. Overman, J. Zhong, and R.M. Lazaro for discussion and assistance.

References

1. Cramer SC. Repairing the human brain after stroke: I. Mechanisms of spontaneous recovery. Ann Neurol. 2008; 63:272–287. [PubMed: 18383072]
2. Brown CE, Aminoltejari K, Erb H, Winship IR, Murphy TH. In vivo voltage-sensitive dye imaging in adult mice reveals that somatosensory maps lost to stroke are replaced over weeks by new structural and functional circuits with prolonged modes of activation within both the peri-infarct zone and distant sites. J Neurosci. 2009; 29:1719–1734. [PubMed: 19211879]
3. Dijkhuizen RM, et al. Correlation between brain reorganization, ischemic damage, and neurologic status after transient focal cerebral ischemia in rats: a functional magnetic resonance imaging study. J Neurosci. 2003; 23:510–517. [PubMed: 12533611]
4. Dobkin BH. Training and exercise to drive poststroke recovery. Nat Clin Pract. 2008; 4:76–85.
5. Carmichael ST. Cellular and molecular mechanisms of neural repair after stroke: making waves. Ann Neurol. 2006; 59:735–742. [PubMed: 16634041]
6. Nudo RJ. Mechanisms for recovery of motor function following cortical damage. Curr Opin Neurobiol. 2006; 16:638–644. [PubMed: 17084614]
7. Alonso-Alonso M, Fregni F, Pascual-Leone A. Brain stimulation in poststroke rehabilitation. Cerebrovasc Dis. 2007; 24(Suppl 1):157–166. [PubMed: 17971652]
8. Di Lazzaro V, et al. Motor Cortex Plasticity Predicts Recovery in Acute Stroke. Cereb Cortex. 2009; 20:1523–1528. [PubMed: 19805417]
9. Hensch TK. Critical period plasticity in local cortical circuits. Nat Rev Neurosci. 2005; 6:877–888. [PubMed: 16261181]
10. Donoghue JP, Suner S, Sanes JN. Dynamic organization of primary motor cortex output to target muscles in adult rats. II. Rapid reorganization following motor nerve lesions. Exp Brain Res. 1990; 79:492–503. [PubMed: 2340869]
11. Foeller E, Celikel T, Feldman DE. Inhibitory sharpening of receptive fields contributes to whisker map plasticity in rat somatosensory cortex. J Neurophysiol. 2005; 94:4387–4400. [PubMed: 16162832]
12. Hess G, Aizenman CD, Donoghue JP. Conditions for the induction of long-term potentiation in layer II/III horizontal connections of the rat motor cortex. J Neurophysiol. 1996; 75:1765–1778. [PubMed: 8734579]
13. Glykys J, Mody I. Hippocampal network hyperactivity after selective reduction of tonic inhibition in GABA A receptor alpha5 subunit-deficient mice. J Neurophysiol. 2006; 95:2796–2807. [PubMed: 16452257]
14. Walker MC, Semyanov A. Regulation of excitability by extrasynaptic GABA(A) receptors. Results Probl Cell Differ. 2008; 44:29–48. [PubMed: 17671772]
15. Collinson N, et al. Enhanced learning and memory and altered GABAergic synaptic transmission in mice lacking the alpha 5 subunit of the GABAA receptor. J Neurosci. 2002; 22:5572–5580. [PubMed: 12097508]
16. Atack JR, et al. L-655,708 enhances cognition in rats but is not proconvulsant at a dose selective for alpha5-containing GABAA receptors. Neuropharmacology. 2006; 51:1023–1029. [PubMed: 17046030]
17. Keros S, Hablitz JJ. Subtype-specific GABA transporter antagonists synergistically modulate phasic and tonic GABAA conductances in rat neocortex. J Neurophysiol. 2005; 94:2073–2085. [PubMed: 15987761]
18. Glykys J, Mody I. Activation of GABAA receptors: views from outside the synaptic cleft. Neuron. 2007; 56:763–770. [PubMed: 18054854]
19. Yoshiike Y, et al. GABA(A) receptor-mediated acceleration of aging-associated memory decline in APP/PS1 mice and its pharmacological treatment by picrotoxin. PLoS One. 2008; 3:e3029. [PubMed: 18716656]
20. Cui Y, et al. Neurofibromin regulation of ERK signaling modulates GABA release and learning. Cell. 2008; 135:549–560. [PubMed: 18984165]

21. Ginsberg MD. Neuroprotection for ischemic stroke: past, present and future. Neuropharmacology. 2008; 55:363–38. [PubMed: 18308347]
22. Que M, Schiene K, Witte OW, Zilles K. Widespread up-regulation of N-methyl-D-aspartate receptors after focal photothrombotic lesion in rat brain. Neurosci Lett. 1999; 273:77–80. [PubMed: 10505620]
23. edecker C, Luhmann HJ, Hagemann G, Fritschy JM, Witte OW. Differential downregulation of GABAA receptor subunits in widespread brain regions in the freeze-lesion model of focal cortical malformations. J Neurosci. 2000; 20:5045–5053. [PubMed: 10864962]
24. Frahm C, et al. Regulation of GABA transporter mRNA and protein after photothrombotic infarct in rat brain. J Comp Neurol. 2004; 478:176–188. [PubMed: 15349978]
25. Neumann-Haefelin T, et al. Immunohistochemical evidence for dysregulation of the GABAergic system ipsilateral to photochemically induced cortical infarcts in rats. Neuroscience. 1998; 87:871–879. [PubMed: 9759975]
26. Kharlamov EA, Downey KL, Jukkola PI, Grayson DR, Kelly KM. Expression of GABA A receptor alpha1 subunit mRNA and protein in rat neocortex following photothrombotic infarction. Brain Res. 2008; 1210:29–38. [PubMed: 18407248]
27. Lee JK, Kim JE, Sivula M, Strittmatter SM. Nogo receptor antagonism promotes stroke recovery by enhancing axonal plasticity. J Neurosci. 2004; 24:6209–6217. [PubMed: 15240813]
28. Tanaka Y, Furuta T, Yanagawa Y, Kaneko T. The effects of cutting solutions on the viability of GABAergic interneurons in cerebral cortical slices of adult mice. J Neurosci Methods. 2008; 171:118–125. [PubMed: 18430473]
29. Baskin YK, Dietrich WD, Green EJ. Two effective behavioral tasks for evaluating sensorimotor dysfunction following traumatic brain injury in mice. J Neurosci Methods. 2003; 129:87–93. [PubMed: 12951236]
30. Ohab JJ, Fleming S, Blesch A, Carmichael ST. A neurovascular niche for neurogenesis after stroke. J Neurosci. 2006; 26:13007–13016. [PubMed: 17167090]

Methods References

31. Glykys J, Mann EO, Mody I. Which GABA(A) receptor subunits are necessary for tonic inhibition in the hippocampus? J Neurosci. 2008; 28:1421–6. [PubMed: 18256262]
32. Verheugen JA, Fricker D, Miles R. Noninvasive measurements of the membrane potential and GABAergic action in hippocampal interneurons. J Neurosci. 1999; 19:2546–2555. [PubMed: 10087068]
33. Barlow R. Cumulative frequency curves in population analysis. Trends Pharmacol Sci. 1990; 11:404–406. [PubMed: 2256180]
34. Baskin YK, Dietrich WD, Green EJ. Two effective behavioral tasks for evaluating sensorimotor dysfunction following traumatic brain injury in mice. J Neurosci Methods. 2003; 129:87–93. [PubMed: 12951236]
35. Schallert T, Fleming SM, Leasure JL, Tillerson JL, Bland ST. CNS plasticity and assessment of forelimb sensorimotor outcome in unilateral rat models of stroke, cortical ablation, parkinsonism and spinal cord injury. Neuropharmacology. 2000; 39:777–787. [PubMed: 10699444]
36. Moore CS, Hebb AL, Blanchard MM, Crocker CE, Liston P, Korneluk RG, Robertson GS. Increased X-linked inhibitor of apoptosis protein (XIAP) expression exacerbates experimental autoimmune encephalomyelitis (EAE). J Neuroimmunol. 2008; 203:79–93. [PubMed: 18687476]

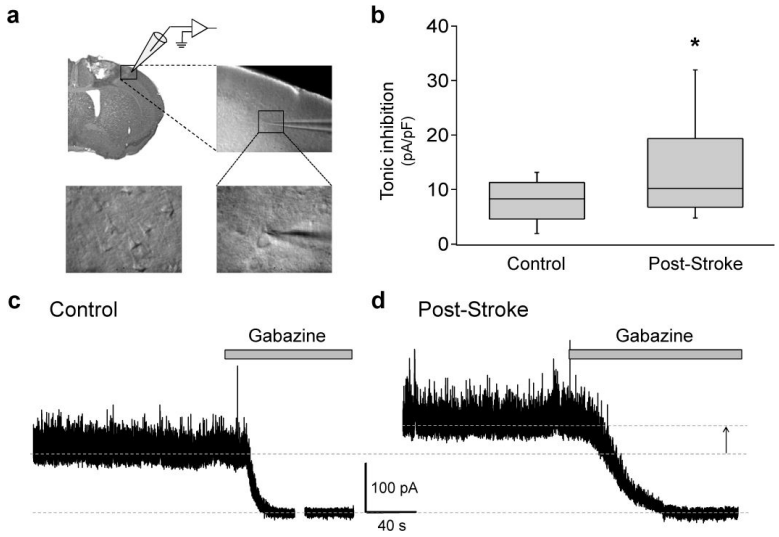

Figure 1. Elevated tonic inhibition in peri-infarct cortex

a, Images showing the peri-infarct recording site. Whole-cell patch-clamp recordings were made from post-stroke brain slices, within 200μm of infarct (top left), from layer-2/3 (top right) pyramidal neurons (bottom panels). **b,** Box-plot (boxes: 25–75%, whiskers:10–90%, lines: median) showing significantly elevated tonic inhibition in peri-infarct cortex (asterisk: $P<0.05$; see Supplementary Fig. 2 for additional analyses). **c,d,** Representative traces showing tonic inhibitory currents in control and peri-infarct neurons, respectively. Tonic currents were revealed by the shift in holding currents after blocking all $GABA_A$Rs with gabazine (>100μM). Cells were voltage-clamped at +10mV.

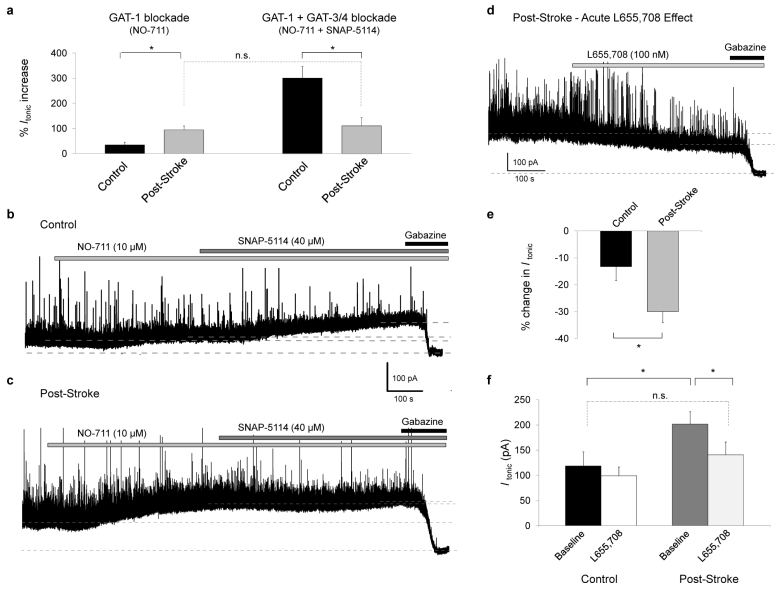

Figure 2. Post-stroke impairment in GABA transport and effect of blocking α5-GABA$_A$Rs

a, Blocking GAT-1 (NO-711) produced a higher % increase in I_{tonic} after stroke; combined blockade of GAT-1 and GAT-3/4 (NO-711 + SNAP-5114) produced a substantial I_{tonic} increase in controls but only an increase equivalent to blocking GAT-1 alone after stroke. **b,c,** I_{tonic} in sequential drug applications. Note the lack of response to SNAP-5114 application in the post-stroke slice. **d**, L655,708 reduced I_{tonic}. **e**, L655,708 significantly decreased post-stroke I_{tonic}. **f**, Drug treatment reverted post-stroke I_{tonic} to near-control level (asterisk: $P<0.05$; n.s.: no significance, bar graphs represent mean ± s.e.m.).

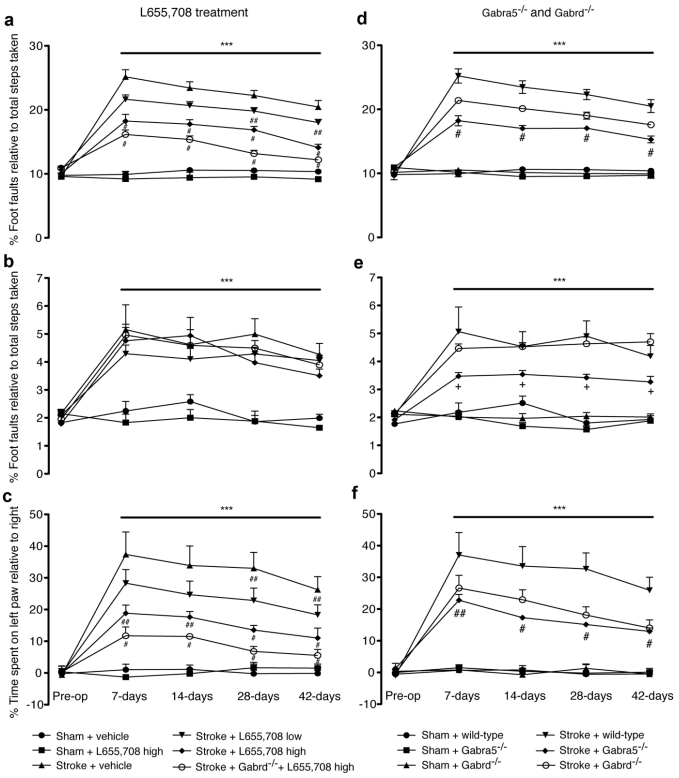

Figure 3. Behavioral recovery after stroke with L655,708 treatment and in Gabra5$^{-/-}$and Gabrd$^{-/-}$ animals

a–**c**, L655,708 treatment starting from 3-days post-stroke resulted in a dose-dependent improvement in functional recovery post-stroke. **d**–**f**, Gabra5$^{-/-}$ and Gabrd$^{-/-}$ mice also showed decreased motor deficits post-stroke. Functional recovery was assessed with forelimb (**a, d**) and hindlimb foot-faults (**b, e**), and on the forelimb asymmetry (**c, f**). Low-dose L655,708 = 200μg/kg/day per animal; high-dose L655,708 = 400μg/kg/day per animal. Data are ± s.e.m. *** = $P \leq 0.001$ stroke + vehicle vs Sham; + = $P \leq 0.05$, ## = $P \leq 0.01$, # = $P \leq 0.001$ vs stroke + vehicle.

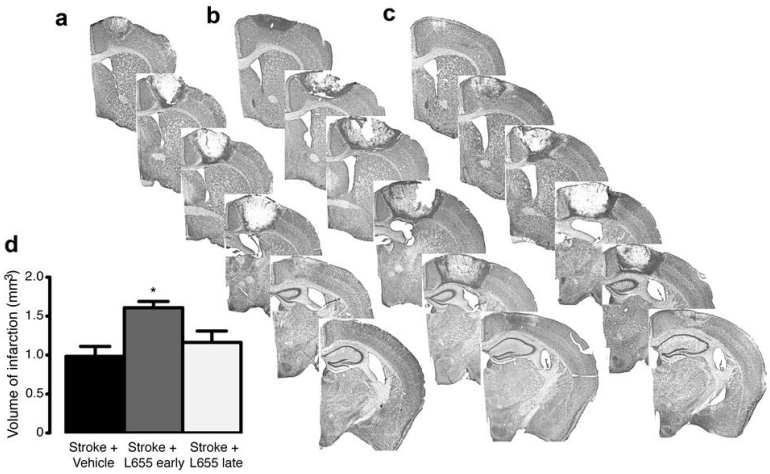

Figure 4. Inflection point in L655,708 treatment effect on infarct size

Representative Nissl stained sections at 7-days post-stroke from stroke + vehicle-treatment (**a**), stroke + L655,708-treatment starting at the time of stroke (**b**) and stroke + L655,708-treatment starting from 3-days post-insult (**c**). Quantification of the stroke volume is shown in panel (**d**). Data are mean ± s.e.m. for n=4 per group, * = $P \leq 0.05$.